Letter

Mpemba effect in pure spin systems : A universal picture of the role of spatial correlations at initial states

Sohini Chatterjee,[1] Soumik Ghosh,[1] Nalina Vadakkayil,[1,2] Tanay Paul,[1] Sanat K. Singha,[1,3] and Subir K. Das[1,*]

[1]*Theoretical Sciences Unit and School of Advanced Materials, Jawaharlal Nehru Centre for Advanced Scientific Research, Jakkur P.O., Bangalore 560064, India*

[2]*Complex Systems and Statistical Mechanics, Department of Physics and Materials Science, University of Luxembourg, Luxembourg, L-1511, Luxembourg*

[3]*Assam Energy Institute, A Centre of Rajiv Gandhi Institute of Petroleum Technology, Sivasagar 785697, India*

(Received 1 February 2024; accepted 3 July 2024; published 25 July 2024)

The quicker freezing of hotter water, than a colder sample, when quenched to a common lower temperature, is referred to as the Mpemba effect (ME). While this counter-intuitive fact remains a surprize since long, efforts have begun to identify similar effect in other systems. We investigate the ME in a rather general context concerning magnetic phase transitions. From Monte Carlo simulations of model systems, viz., the Ising model and the q-state Potts model, with varying range of interaction and space dimension, we assert that hotter paramagnets undergo ferromagnetic ordering faster than the colder ones. This conclusion we have arrived at following the analyses of the simulation results on decay of energy and growth in ordering following quenches from different starting temperatures, to fixed final temperatures below the Curie points. The general observation, in all the considered models, without any element of frustration, is a crucial and important fact of our study. Furthermore, we have obtained an important scaling picture, on the strength of the effect, with respect to the variation in spatial correlation in the initial states. This behavior appears true irrespective of the nature of order-parameter fluctuation and even order of transition. The observations are expected to be relevant to the understanding of ME in a rather general class of systems.

DOI: 10.1103/PhysRevE.110.L012103

If two bodies of liquid water, differing in temperature, are placed inside a refrigerator, operating at a subzero temperature ($<0^\circ$ C), the most common prediction will be that the colder one will freeze faster. The report by Mpemba and Osborne [1], however, contradicts this expectation. There is a surge [1–32] in interest in understanding this counterintuitive fact, which was also mentioned by Aristotle [33], now referred to as the Mpemba effect (ME). Recently, questions relevant to the ME are posed in more general ways [2]: When two samples of the same material, from two different temperatures, are quenched to a common lower temperature, which one will reach the new equilibrium quicker? If there exists a point of phase transition, between the final and the initial temperatures, for which starting temperature will the transformation occur earlier? Experimental studies of colloidal systems [10], clathrate hydrates [11], carbon nanotube resonators [12], and magnetic alloys [13] show the presence of ME. In the theoretical literature, the studied varieties [34–37] include granular matter [14–17], spin glass [18], and few other systems of magnetic origin [19–22]. Nevertheless, the underlying reason(s) remains a puzzle. The pertaining new questions are fundamental from several theoretical angles. Answers to these may be exploited to much practical advantage [28].

Nucleation is strongly influenced by metastability [38], for which the choices of the final temperature (T_f), the type and the volume fraction of impurity, etc., matter. How the role of the starting temperature (T_s) enters the picture is an important new fundamental issue. Is it that the above mentioned metastable aspect gets affected by the nature of the initial thermodynamic state in an unexpected order? With in-built frustration, some of the works perhaps set the objective of exploring this angle. Interestingly, adding to the puzzle, even the standard ferromagnetic Ising model, without any impurity, is seen to exhibit the effect [21]. To understand the reason, it is important to study the model in other situations, e.g., in different space dimensions (d) and with varying range of interactions. Crucially, it should be checked what are the effects of the order of transitions [2,22,29]. Note that, for water, the transition is of first order character, while for the Ising model the problem was designed [21] to capture the influence of a second order transition. Here we chose the q-state Potts model [37,39], for which the order of transition varies with q.

Interestingly, we observe the ME in all the above cases. There exists similar experimental report [13], though in the latter magnetic case, primary reason was related to glassy ingredients. This and other works make our finding more interesting and the effect more general. Note that none of our systems possess frustration or glassy features. Furthermore, we observe interesting scaling with respect to spatial correlation in the initial states. This is valid not only for the simple variation of q, but also with the change of the order of transition, space dimension, and critical fluctuation. These results are of much experimental relevance and can potentially

*Contact author: das@jncasr.ac.in

provide crucial insights to the interpretation of ME in a broad variety of systems.

As already mentioned, here we study a class of discrete spin systems with pure ferromagnetic interactions. We investigate the Ising model [37] in different dimensions, having short and long-range intersite potentials [40]. Furthermore, generalization of this two-component system into multicomponent ones have also been considered. In general, the Hamiltonian can be written as $H = -\sum_{i(\neq)j} J(r_{ij})\delta_{S_i,S_j}$; $S_i, S_j = 1, 2, ..., q$; r_{ij} being the separation between lattice sites i and j. For $q = 2$, this Potts model Hamiltonian corresponds to the Ising model, differing only by a factor of two. The latter, by correcting for the factor, we have studied in $d = 2$ and 3, with nearest neighbor (NN) interactions, by setting the interaction strength J to unity, on square and simple cubic lattices, respectively. In $d = 2$, we have also presented results for the long-range (LR) version of the Ising model with [40] $J(r_{ij}) = 1/r_{ij}^{2+\sigma}$, for $\sigma = 0.8$, again using the square lattice. Most extensive results are obtained for the Potts model, q varying between two and ten. The critical temperature for this model has the q-dependence [37] $T_c = J/[k_B \ln(1 + \sqrt{q})]$, k_B being the Boltzmann constant, to be set to unity. Depending on the value of q, the order of transition can alter. For $q > 4$ the model loses its "critical" character [39], the transition being of first order. For the Ising case, the values of T_c in $d = 2$ and 3 are $\simeq 2.269\, J/k_B$ and $\simeq 4.51\, J/k_B$, respectively [37]. For the long-range case we have used [41] $T_c = 9.765\, J/k_B$.

The kinetics of transition for instantaneous quenches, of systems in periodic $L \times L$ boxes, like some other works [18,21], from para to ferro regions, starting with equal fractions of all spin states, are studied via Monte Carlo simulations [37], with the Glauber spin-turn mechanism [37]. The preparation of the initial configurations near a T_c encounters critical slowing down [37]. To avoid this, we have used cluster algorithms. In the case of short-range Ising or Potts models, this is done by implementing the Wolff algorithm [42], and for the LR Ising model, we have used the Fukui-Todo algorithm [41,43]. The presence of the correlated spatial fluctuations in a system and its variation with temperature can be quantified via the calculation of the structure factor: $S(k, t) = \langle \psi_k(t)\, \psi_{-k}(t) \rangle$, $\psi_k(t)$ being the Fourier transform of the order parameter [44] $\psi(\vec{r}, t)$ $(= \exp(i\,\theta(\vec{r}))$; $\theta = 2\pi n/q$, $n = 1, \ldots, q)$. In the small wave number (k) regime [$\in (0, 0.4)$ or shorter], for the short-range cases, $S(k, t)$ is described well by the Ornstein-Zernike relation [45,46], $S(k) = k_B\, T_s\, \chi/(1 + k^2\, \xi^2)$, χ being the susceptibility and ξ the correlation length. The average length, $\ell(t)$, of the clusters of up or down spins, during an evolution toward a ferromagnetic state, has been estimated via the first moment of the domain size distribution function [47], $P(\ell_d)$, i.e., $\ell(t) = \int P(\ell_d, t)\ell_d d\ell_d$, where ℓ_d is the distance between two consecutive domain interfaces along a given direction. Unless mentioned, we used $L = 256$.

In Fig. 1 we depict how the choice of T_s, in the case of the Potts model, can influence the structural features in the initial configurations, for different values of q. For both the considered cases, viz., $q = 2$ and 5, the configurations at higher T_s [see the snapshots at the bottom of the columns in (a) and (b)] appear random or structureless. With the decrease of T_s, spatial correlations emerge. This is more clearly identifiable in the case of $q = 2$ for which one expects the critical

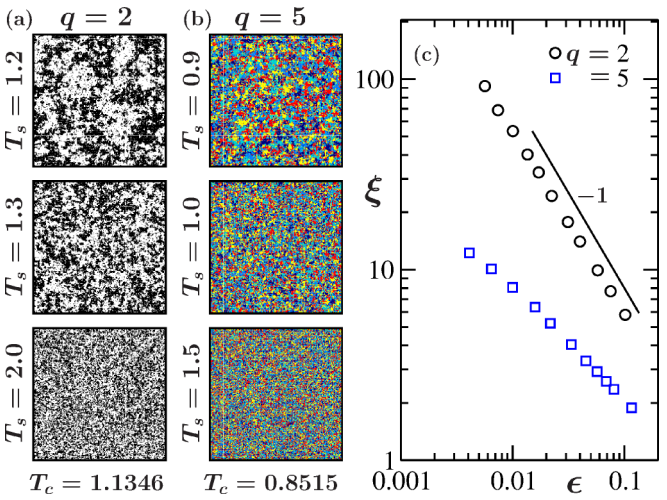

FIG. 1. Typical equilibrium configurations, for $q = 2$ and 5 state Potts models, are shown in (a) and (b) from different starting temperatures T_s, located above the respective critical temperatures T_c. (c) Plots of the correlation lengths, ξ, versus ϵ $(= (T_s - T_c)/T_c)$, for the same Potts models. For $q = 2$, ξ diverges as $\epsilon^{-\nu}$, with $\nu = 1$ (see the solid line).

divergence [45,46] $\xi \sim \epsilon^{-\nu}$, with $\nu = 1$. For a wide range of ϵ $(= |T_s - T_c|/T_c)$ such a behavior can be appreciated from Fig. 1(c). For $q = 5$, the phase transition is of first order [39], and we do not associate any exponent with the data set. The enhancement in the value of ξ can be appreciated for this q as well. In this case, the bending on the log-log scale over an extended range can well be, in addition to the finite-size effects, due to the first-order nature of the transition. Our expectation is that for such high q the ME will be weaker. We proceed with the objective of quantifying it and to investigate if there exists any scaling rule [2] for arbitrary q that can also comply with the other considered models.

We quench the systems from different [48] T_s to $T_f = 0.5\, T_c$, for a large set of q values. In Fig. 2 we show results obtained during evolutions following such quenches for the 5-state Potts model. In parts (a) and (b) we show the snapshots at different stages of evolutions for $T_s = 0.9$ and 1.1, respectively. It is evident that the system from the higher T_s reaches the final equilibrium faster. This comparative picture is true not only for the chosen set of initial configurations: the trend of faster approach to equilibrium stands correct for an overwhelmingly large number of the combinations of starting configurations. In part (c) we look at the decay of the average energy (E) of the systems during the relaxation processes. Unlike certain other cases, see, e.g., Ref. [18], energy for the considered models and protocol appears a monotonic function of time. Thus, comparisons of this quantity at early and late enough times, for different T_s, should help appropriately identify the ME. We have included results for a few T_s in Fig. 2(c). Each of the data sets is presented after averaging over 300 000 independent initial configurations. For clarity, we have enlarged the early and late time behavior separately, in the upper and lower panels, respectively. The orders of appearances of the plots, in terms of T_s, are systematic and opposite in the two panels. This implies that there are

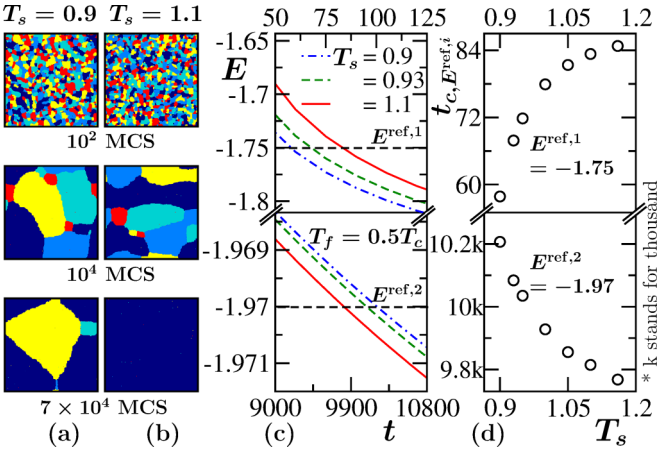

FIG. 2. Demonstration of relaxation in the 5-state Potts model, following quenches to $T_f = 0.5\,T_c$, from different T_s, starting with equal fractions of different spin states. In (a) and (b) we show evolution snapshots, taken at different times, in units of standard Monte Carlo steps, for the systems initially at (a) $T_s = 0.9$ and (b) $T_s = 1.1$. Different colors represent q different Potts states. (c) Plots of energy versus time, following quenches from several T_s values. See text for the dashed lines and the broken frame. (d) Plots of $t_{c,E^{\mathrm{ref},1}}$ (upper panel) and $t_{c,E^{\mathrm{ref},2}}$ (lower panel), versus T_s.

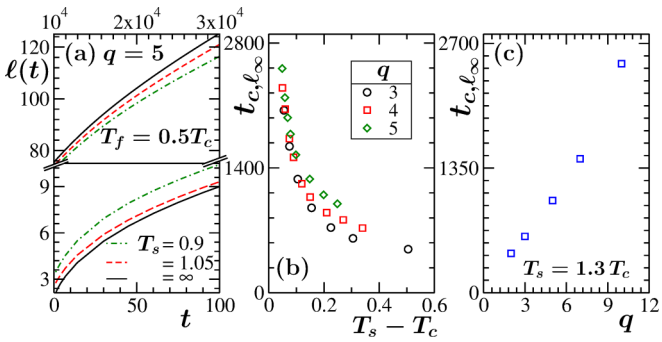

FIG. 3. (a) Plots of $\ell(t)$ versus t, for the 5-state Potts model, for quenches from various T_s to $T_f = 0.5\,T_c$. (b) Plots of time, t_{c,ℓ_∞}, corresponding to crossing between growth curves for systems starting at $T_s = \infty$ and a finite T_s, as a function of $T_s - T_c$, for different q values. (c) Plot of t_{c,ℓ_∞} versus q, for systems prepared at $T_s = 1.3\,T_c$.

crossings amongst the energy curves, due to faster equilibrations of configurations prepared at higher T_s. This is the essence of the Mpemba effect [1,2,18,21]. For a clear demonstration of a strong systematicity, we perform the following exercise. The dashed horizontal lines in these panels correspond to two reference energy values, $E^{\mathrm{ref},1}$ and $E^{\mathrm{ref},2}$. We calculate the crossing time between a dashed line and the energy curve of the systems starting from each of the T_s values. Such a crossing time is denoted by $t_{c,E^{\mathrm{ref},i}}$, $i = 1, 2$. Part (d) of Fig. 2 shows $t_{c,E^{\mathrm{ref},i}}$ as a function of T_s. The early time quantity (upper panel), i.e., $t_{c,E^{\mathrm{ref},1}}$, increases with the increase in T_s, but at late times (lower panel) we see a different behavior, i.e., $t_{c,E^{\mathrm{ref},2}}$ decreases with the increase in T_s. This implies faster relaxation of the systems with higher T_s, indicating the presence of ME.

The faster relaxation of the higher T_s systems can also be quantified by calculating the average domain length, $\ell(t)$, a key probe for investigating coarsening dynamics [47–49]. In Fig. 3(a), we plot $\ell(t)$ vs t, for different T_s values, for $q = 5$. The early time behavior for different T_s are presented in the lower part of the divided graph. The late time comparisons are in the upper part. The systems starting at higher T_s tend to approach the new equilibrium earlier. This conveys a picture the same as that derived from the energy decay, further strongly suggesting the presence of the Mpemba effect. We record the times at which the domain lengths of the systems for different finite T_s ($< \infty$) values are crossed or overtaken by the corresponding plots for the systems starting from $T_s = \infty$. We denote this by t_{c,ℓ_∞}. In Fig. 3(b) we have plotted t_{c,ℓ_∞} as a function of $T_s - T_c$, for a few values of q, covering transitions of first, as well as second order varieties. For each q, the crossing time increases with the approach of T_s to the corresponding T_c. Eventually, however, the plot for $T_s = \infty$ overtakes those for all the considered lower values of T_s. The same scenario applies to a reference $T_s < \infty$. This implies that systems from all T_s values tend to approach new equilibrium quicker than the systems starting from any lower T_s. While this conclusion appears true for the presented cases, general validity requires more sophisticated study and analysis.

Given that, depending upon the value of q the nature of critical fluctuation is different, presence of any unique scaling behavior may not emerge from Fig. 3(b). It appears, nevertheless, that for a given distance of T_s from T_c, the crossing time is longer for higher q. A quantitative picture for this is shown in Fig. 3(c). This is a signature that the ME gets weaker with the increase of q. Considering the influence of both q and T_s, the issue, however, is complex. Nevertheless, if a scaling picture, as desired above, can be drawn, crucial identification of the presence or strength of the effect can be made irrespective of the nature of critical fluctuation and order of transition. We will return to this important objective later.

Now we check whether the same scenario is true for the case of the LR Ising model. Due to the demanding computation, we analyze results for this case after averaging over 100 independent initial configurations. Note that the LR systems encounter finite-size effects much faster than its short-range counterpart, due to faster growth [40,50,51] with the decrease of σ. To avoid this problem, we choose big systems and a large value of σ, viz., $\sigma = 0.8$, which, nevertheless, falls well within the long-range interaction domain [40]. In Fig. 4(a) we plot $\ell(t)$ vs t, for quenches to $T_f = 0.3\,T_c$, from three T_s values, with $L = 1024$. From these plots it is clear that the systems with the highest T_s have the largest $\ell(t)$ at late times. Thus, ME appears to be present in the LR Ising model as well. Note that because of the above mentioned reasons we have used Ewald summation [41,52], and parallelized our codes, in this case, to speed up the output.

It should be noted that in equilibrium critical phenomena the LR Ising model possesses values of exponents that are the same as those from the mean-field theory [45,46] for the short-range Ising model. Thus, one may ask, if our study confirms ME in the corresponding mean-field dynamical model with the same quantitative scaling features, if any, as the actual Ising model that we further investigate below. It is worth mentioning that there exist studies in the literature [22,26,29–

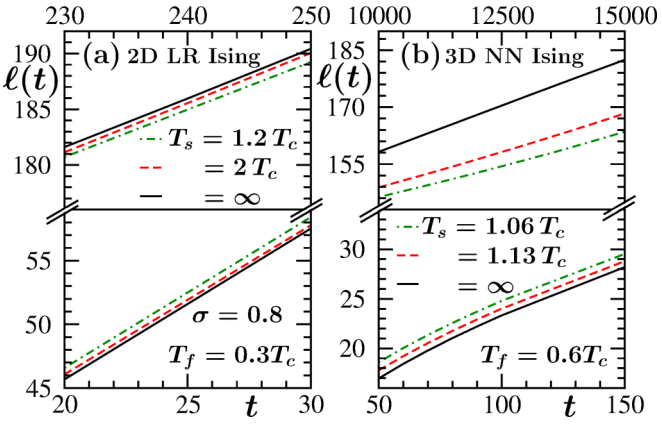

FIG. 4. (a) Plots of $\ell(t)$ versus t, corresponding to a few different T_s values, for quenches to $0.3\,T_c$, for the LR Ising model. The value of σ is 0.8 and we have $L = 1024$. (b) Same as (a) but here the results are for the 3D nearest-neighbor (NN) Ising model with $T_f = 0.6\,T_c$ and $L = 256$.

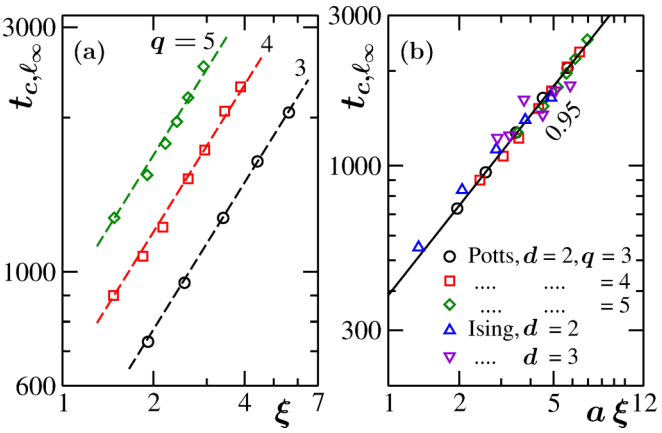

FIG. 5. (a) Plots of t_{c,ℓ_∞} versus ξ, for the Potts model, with a few different q values, on a double-log scale. (b) Same as (a) but here the abscissa of the data sets are scaled by constant factors to obtain a "possible" overlap. In addition to the results from the Potts cases ($q \geqslant 3$), here we have included data for the NN Ising model, from different space dimensions. While presenting the results, we tried to avoid finite-size effects very close to T_c and corrections to critical scaling by staying within 25% from T_c. Dashed and solid lines represent power laws.

31] that report ME in mean field models. However, even if the protocols and dynamical rules match with our studies, e.g., those for an antiferromagnetic system in Ref. [30], it is important to note certain interesting facts. As opposed to the case of exponents in equilibrium critical phenomena, the mean-field Ginzburg-Landau approach for the ferromagnetic model provides the same asymptotic growth exponent [53] as the one obtained from MC simulations of the short-range Ising model. Adding to the anomaly, interestingly, for the LR Ising case the value of this exponent depends further upon microscopic details of the range of the interaction [40,50]. Thus, it is important that one truly visits the mean-field coarsening case, corresponding to the short-range ferromagnetic Ising model, to make a very general remark on the scaling features in ME against the interplay between critical and coarsening behavior, that we discuss further below.

So far we have dealt with 2D systems. Now we present results from the 3D NN Ising model in Fig. 4(b), where the faster relaxation of the systems for the higher T_s value is also quite clear. Here we have quenched the systems from different initial T_s values to $T_f = 0.6\,T_c$. These results are presented after averaging over runs with 2880 independent initial configurations, with $L = 256$.

Returning to the Potts results in Fig. 3, we recall that an important objective of our work is to obtain a scaling picture [2]. Note that for different q values, one expects differing fluctuations in the critical vicinity. Thus, as stated above, a unique behavior of the data sets in Fig. 3(b) may not be expected. It is possibly more instructive to replace the abscissa variable there by ξ. Results from such an exercise are shown in Fig. 5(a). On a log-log scale it appears that the data sets from different q are reasonably parallel to each other. Thus, in Fig. 5(b), we introduce a prefactor a for the abscissa, constant for a particular value of q, to obtain an overlap of the data sets in Fig. 5(a). A nice collapse of the data sets can be appreciated. In fact, the results for the 2D and 3D Ising models also comply with that. This observation carries important meaning that we describe below. It is worth mentioning here that accurate estimations of the crossing times require huge statistics.

We have investigated the presence of the Mpemba effect [1–5] during para- to ferromagnetic transitions in model systems with discrete spin values. These include short-range Ising models in $d = 2$ and 3, as well as long-range Ising models in $d = 2$. A very extensive set of results are presented for the q-state Potts model for a wide range of q values. It is important to note that in none of the considered models there exist in-built frustration. Despite that, very interestingly, irrespective of the space dimension, range of interaction, and order of transition, we have observed the ME. It has an important connection with the extent of spatial correlations at the considered initial temperatures. The relative delay in approach to the final equilibrium, following quenches from para to ferro regions, with the lowering of starting temperatures, has reasonably unique dependence upon ξ. For second order transitions we have observed this scaling feature for models with critical exponent ν varying nearly by a factor of 1.6. Furthermore, the power-law scaling appears valid even for a first order transition. The value of the exponent ($\simeq 1$) connecting the crossing times and ξ, in Fig. 5(b), implies that the evolution during early transients gets severely slower as $T_s \to T_c$. This may be [2] because of the conversion of fractality associated with the initial correlation to that of the domain morphology at the early periods. It will be interesting [2] to investigate how certain exponents from dynamic critical phenomena [54] may influence this feature. The overall picture also signifies, for a given model, if two initial temperatures possess nearly the same spatial correlations, possible for large q, configurations from these states will equilibrate almost simultaneously at the final temperature, showing no detectable ME, even for large differences in the T_s.

It will be interesting to compare the phase transition times for various T_s values [22]. Note that here we compared,

instead, the rates of ordering that lead to the identifications of ME via crossings of relaxation trajectories. This way our identification is of a variety similar to those in Refs. [10,14–19]. We have used the Metropolis algorithm in this work. A preliminary study with the Glauber transition rate, like in Ref. [30] for the antiferromagnetic case, also suggests presence of ME in our 2D ferromagnetic Ising model. In the future it will be interesting to confirm ME in other models as well, for the latter transition rate. We intend also to undertake studies of boundary effects as in Ref. [32].

S.K.D. acknowledges a discussion with R. Pandit at an early stage and partial financial support from Science and Engineering Research Board, India, via Grant No. MTR/2019/001585. The authors are thankful to the supercomputing facility, PARAM Yukti, at JNCASR, under National Supercomputing Mission.

[1] E. B. Mpemba and D. G. Osborne, Cool? Phys. Educ. **4**, 172 (1969).
[2] S. K. Das, Perspectives on a few puzzles in phase transformations: When should the farthest reach the earliest? Langmuir **39**, 10715 (2023).
[3] J. Bechhoefer, A. Kumar, and R. Chétrite, A fresh understanding of the Mpemba effect, Nat. Rev. Phys. **3**, 534 (2021).
[4] D. Auerbach, Supercooling and the Mpemba effect: When hot water freezes quicker than cold, Am. J. Phys. **63**, 882 (1995).
[5] M. Jeng, The Mpemba effect: When can hot water freeze faster than cold? Am. J. Phys. **74**, 514 (2006).
[6] X. Zhang *et al.*, Hydrogen-bond memory and water-skin supersolidity resolving the Mpemba paradox, Phys. Chem. Chem. Phys. **16**, 22995 (2014).
[7] J. Jin and W. A. Goddard III, Mechanisms underlying the Mpemba effect in water from molecular dynamics simulations, J. Phys. Chem. C **119**, 2622 (2015).
[8] Y. Tao, W. Zou, J. Jia, W. Li, and D. Cremer, Different ways of hydrogen bonding in water - why does warm water freeze faster than cold water? J. Chem. Theory Comput. **13**, 55 (2017).
[9] Z. Tang, W. Huang, Y. Zhang, Y. Liu, and L. Zhao, Direct observation of the Mpemba effect with water: Probe the mysterious heat transfer, InfoMat **5**, e12352 (2023).
[10] A. Kumar and J. Bechhoefer, Exponentially faster cooling in a colloidal system, Nature (London) **584**, 64 (2020).
[11] Y.-H. Ahn, H. Kang, D.-Y. Koh, and H. Lee, Experimental verifications of Mpemba-like behaviors of clathrate hydrates, Korean J. Chem. Eng. **33**, 1903 (2016).
[12] P. A. Greaney, G. Lani, G. Cicero, and J. C. Grossman, Mpemba-like behavior in carbon nanotube resonators, Metall. Mater. Trans. A **42**, 3907 (2011).
[13] P. Chaddah, S. Dash, K. Kumar, and A. Banerjee, Overtaking while approaching equilibrium, arXiv:1011.3598.
[14] A. Lasanta, F. V. Reyes, A. Prados, and A. Santos, When the hotter cools more quickly: Mpemba effect in granular fluids, Phys. Rev. Lett. **119**, 148001 (2017).
[15] A. Torrente, M. A. López-Castaño, A. Lasanta, F. V. Reyes, A. Prados, and A. Santos, Large Mpemba-like effect in a gas of inelastic rough hard spheres, Phys. Rev. E **99**, 060901(R) (2019).
[16] A. Biswas, V. V. Prasad, O. Raz, and R. Rajesh, Mpemba effect in driven granular Maxwell gases, Phys. Rev. E **102**, 012906 (2020).
[17] R. Gómez González and V. Garzó, Time-dependent homogeneous states of binary granular suspensions, Phys. Fluids **33**, 093315 (2021).
[18] M. Baity-Jesi *et al.*, The Mpemba effect in spin glasses is a persistent memory effect, Proc. Natl. Acad. Sci. USA **116**, 15350 (2019).
[19] Z. Lu and O. Raz, Nonequilibrium thermodynamics of the Markovian Mpemba effect and its inverse, Proc. Natl. Acad. Sci. USA **114**, 5083 (2017).
[20] A. Gal and O. Raz, Precooling strategy allows exponentially faster heating, Phys. Rev. Lett. **124**, 060602 (2020).
[21] N. Vadakkayil and S. K. Das, Should a hotter paramagnet transform quicker to a ferromagnet? Monte Carlo simulation results for Ising model, Phys. Chem. Chem. Phys. **23**, 11186 (2021).
[22] R. Holtzman and O. Raz, Landau theory for the Mpemba effect through phase transitions, Commun Phys **5**, 280 (2022).
[23] A. Biswas, R. Rajesh, and A. Pal, Mpemba effect in a Langevin system: Population statistics, metastability, and other exact results, J. Chem. Phys. **159**, 044120 (2023).
[24] M. R. Walker and M. Vucelja, Anomalous thermal relaxation of Langevin particles in a piecewise-constant potential, J. Stat. Mech.: Theory and Expt. (2021) 113105.
[25] M. Vynnycky and S. Kimura, Can natural convection alone explain the Mpemba effect? Int. J. Heat Mass Transf. **80**, 243 (2015).
[26] Z. Y. Yang and J.-X. Hou, Mpemba effect of a mean-field system: The phase transition time, Phys. Rev. E **105**, 014119 (2022).
[27] F. J. Schwarzendahl and H. Löwen, Anomalous cooling and overcooling of active colloids, Phys. Rev. Lett. **129**, 138002 (2022).
[28] Z. Cao, R. Bao, J. Zheng, and Z. Hou, Fast functionalization with high performance in the autonomous information engine, J. Phys. Chem. Lett. **14**, 66 (2023).
[29] S. Zhang and J.-X. Hou, Theoretical model for the Mpemba effect through the canonical first-order phase transition, Phys. Rev. E **106**, 034131 (2022).
[30] I. Klich, O. Raz, O. Hirschberg, and M. Vucelja, Mpemba index and anomalous relaxation, Phys. Rev. X **9**, 021060 (2019).
[31] Z.-Y. Yang and J.-X. Hou, Non-Markovian Mpemba effect in mean-field systems, Phys. Rev. E **101**, 052106 (2020).
[32] G. Teza, R. Yaacoby, and O. Raz, Relaxation shortcuts through boundary coupling, Phys. Rev. Lett. **131**, 017101 (2023).
[33] Aristotle, *Meteorologica*, translated by H. D. P. Lee (Harvard University Press, 1952), Book I, Chap. XII, pp. 85–87.
[34] N. V. Brilliantov and T. Pöschel, *Kinetic Theory of Granular Gases* (Oxford University Press, Oxford, 2004).
[35] H. J. Herrmann, J.-P. Hovi, and S. Luding, eds. *Physics of Dry Granular Media* (Springer Science & Business Media, 2013), Vol. 350.

[36] K. Binder and A. P. Young, Spin glasses: Experimental facts, theoretical concepts, and open questions, Rev. Mod. Phys. **58**, 801 (1986).

[37] D. P. Landau and K. Binder, *A Guide to Monte Carlo Simulations in Statistical Physics* (Cambridge University Press, Cambridge, 2009).

[38] M. Matsumoto, S. Saito, and I. Ohmine, Molecular dynamics simulation of the ice nucleation and growth process leading to water freezing, Nature (London) **416**, 409 (2002).

[39] K. Binder, Static and dynamic critical phenomena of the two-dimensional q-state Potts model, J. Stat. Phys. **24**, 69 (1981).

[40] A. J. Bray, Domain-growth scaling in systems with long-range interactions, Phys. Rev. E **47**, 3191 (1993).

[41] T. Horita, H. Suwa, and S. Todo, Upper and lower critical decay exponents of ising ferromagnets with long-range interaction, Phys. Rev. E **95**, 012143 (2017).

[42] U. Wolff, Collective Monte Carlo updating for spin systems, Phys. Rev. Lett. **62**, 361 (1989).

[43] K. Fukui and S. Todo, Order-N cluster Monte Carlo method for spin systems with long-range interactions, J. Comput. Phys. **228**, 2629 (2009).

[44] S. Puri, R. Ahluwalia, and A. J. Bray, Dynamical crossover in the clock model with a conserved order parameter, Phys. Rev. E **55**, 2345 (1997).

[45] M. E. Fisher, The theory of equilibrium critical phenomena, Rep. Prog. Phys. **30**, 615 (1967).

[46] H. E. Stanley, *Introduction to Phase Transitions and Critical Phenomena* (Clarendon Press, Oxford, 1971).

[47] S. Majumder and S. K. Das, Diffusive domain coarsening: Early time dynamics and finite-size effects, Phys. Rev. E **84**, 021110 (2011).

[48] S. Chakraborty and S. K. Das, Role of initial correlation in coarsening of a ferromagnet, Eur. Phys. J. B **88**, 160 (2015).

[49] A. J. Bray, Theory of phase-ordering kinetics, Adv. Phys. **51**, 481 (2002).

[50] H. Christiansen, S. Majumder, and W. Janke, Phase ordering kinetics of the long-range Ising model, Phys. Rev. E **99**, 011301(R) (2019).

[51] S. Ghosh and S. K. Das, Nonuniversal aging during phase separation with long-range interaction, Phys. Rev. E **109**, L052102 (2024).

[52] M. P. Allen and D. J. Tildesley, *Computer Simulation of Liquids* (Oxford University Press, 2017).

[53] S. K. Das, J. Horbach, and K. Binder, Kinetics of phase separation in thin films: Lattice versus continuum models for solid binary mixtures, Phys. Rev. E **79**, 021602 (2009).

[54] U. C. Täuber, *Critical Dynamics: A Field Theory Approach to Equilibrium and Non-Equilibrium Scaling Behavior* (Cambridge University Press, 2014).